SYNTHESIS OF HYDROXYAPATITE VIA SOL-GEL METHOD FOR TOOTH REMINERALIZATION APPLICATIONS

Soni Setiadji[*], Frida Aziz Damayanti[*], Fiona Putri Septiani[*], Agung Wahana[**], Tina Dewi Rosahdi[*]

[*]*Department of Chemistry, Faculty of Science and Technology, UIN Sunan Gunung Djati Bandung, Bandung, Indonesia, s.setiadji@uinsgd.ac.id, fionaps52@gmail.com, tina_dr@uinsgd.ac.id*

[**]*Department of Informatics Engineering, Faculty of Science and Technology, UIN Sunan Gunung Djati Bandung, Bandung, Indonesia, wahana.agung@uinsgd.ac.id*

Email Correspondence: s.setiadji@uinsgd.ac.id

Received : March 12, 2026 Accepted : June 25, 2026 Published : June 30, 2026

Abstract: Enamel, the outermost and most highly mineralized tissue in the human body, is composed predominantly of hydroxyapatite and is susceptible to demineralization under acidic conditions, which can lead to enamel erosion and dental caries. Due to its chemical similarity to natural tooth mineral, hydroxyapatite has been extensively investigated as a biomimetic material for enamel remineralization. This study aimed to synthesize hydroxyapatite via the sol–gel method, formulate it into a hydroxyapatite-based paste, and evaluate its remineralization effect on demineralized premolar enamel. Hydroxyapatite was synthesized through a sol–gel process involving the reaction of $Ca(OH)_2$ and H_3PO_4 at 60 °C followed by pH adjustment, aging, drying, and calcination. The material was characterized using X-ray diffraction (XRD), X-ray fluorescence (XRF), and particle size analysis (PSA). The hydroxyapatite paste was applied once daily for 14 consecutive days to demineralized premolar enamel, and remineralization was evaluated using scanning electron microscopy (SEM). XRD confirmed the formation of the hydroxyapatite phase, XRF indicated a Ca/P ratio of 1.72, and PSA showed an average particle size of 344.2 nm, suggesting the presence of particle agglomeration. SEM analysis demonstrated reduced surface porosity and partial filling of enamel defects after treatment compared to demineralized enamel. This study provides a simple sol–gel synthesis and application approach for hydroxyapatite paste, offering potential relevance for future development of non-invasive enamel repair materials in dental restorative applications.

Keywords: demineralization; hydroxyapatite; nano-hydroxyapatite; remineralization; sol–gel

Abstrak: Enamel, yang merupakan jaringan terluar dan paling termineralisasi tinggi pada tubuh manusia, tersusun secara dominan oleh hidroksiapatit dan rentan mengalami demineralisasi dalam kondisi asam, yang dapat memicu terjadinya erosi enamel dan karies gigi. Karena kemiripan kimianya dengan mineral alami gigi, hidroksiapatit telah diteliti secara luas sebagai material biomimetik untuk remineralisasi enamel. Penelitian ini bertujuan untuk mensintesis hidroksiapatit melalui metode sol–gel, memformulasikannya ke dalam bentuk pasta berbasis hidroksiapatit, serta mengevaluasi efek remineralisasinya pada enamel gigi premolar yang terdemineralisasi. Hidroksiapatit disintesis melalui proses sol–gel yang melibatkan reaksi antara $Ca(OH)_2$ dan H_3PO_4 pada

suhu 60 °C, diikuti dengan penyesuaian pH, aging (penuaan), pengeringan, dan kalsinasi. Karakterisasi material dilakukan menggunakan XRD, XRF, dan PSA. Pasta hidroksiapatit diaplikasikan sekali sehari selama 14 hari berturut-turut pada enamel gigi premolar yang telah terdemineralisasi, dan proses remineralisasinya dievaluasi menggunakan SEM. Hasil XRD mengonfirmasi terbentuknya fase hidroksiapatit, analisis XRF menunjukkan rasio Ca/P sebesar 1,72, dan PSA menunjukkan ukuran partikel rata-rata sebesar 344,2 nm yang mengindikasikan adanya aglomerasi partikel. Analisis SEM menunjukkan penurunan porositas permukaan dan pengisian sebagian pada cacat enamel setelah perlakuan dibandingkan dengan enamel yang terdemineralisasi. Penelitian ini menyediakan pendekatan sintesis sol–gel dan aplikasi yang sederhana untuk pasta hidroksiapatit, serta memberikan relevansi potensial bagi pengembangan material perbaikan enamel non-invasif di masa depan dalam aplikasi restorasi gigi.

Kata kunci: demineralisasi; hidroksiapatit; nano-hidroksiapatit; remineralisasi; sol–gel

Recommended APA Citation:

Setiadji, S., Damayanti, F. A., Septiani, F. P., & Rosahdi, T. D. (2026). Synthesis of Hydroxyapatite Via Sol–Gel Method for Tooth Remineralization Applications. *Elkawnie*, 12(1), 190-202. https://doi.org/10.22373/ekw.v12i1.34419

Introduction

Enamel is the hardest tissue in the human body, composed of approximately 96–97% hydroxyapatite mineral ($Ca_{10}(PO_4)_6(OH)_2$). Despite its high level of mineralization, enamel is susceptible to demineralization caused by exposure to acidic environments from food, beverages, and bacterial metabolic activities in the oral cavity. The demineralization process leads to the release of calcium and phosphate ions from the enamel structure, thereby triggering dental tissue damage, such as caries and enamel erosion (Xu, et al., 2022). Remineralization is required to restore the lost minerals and prevent further progression of enamel damage.

Fluoride remains the most commonly used remineralization agent due to its ability to enhance enamel resistance against acid. However, its effectiveness is primarily limited to early enamel lesions, and long-term use in high concentrations carries the potential risk of causing fluorosis. Consequently, the development of alternative remineralization materials that are more biocompatible and structurally similar to natural enamel has become a major focus in the field of dental biomaterials (Guntermann, Rohrbach, Schäfer, & Dammaschke, 2022; Wierichs, Wolf, Campus, & Carvalho, 2022).

One material with significant potential as a remineralization agent is nano-hydroxyapatite. This material possesses a composition and crystal structure identical to the primary mineral component of enamel, allowing for excellent interaction with dental tissues. At the nanoscale, hydroxyapatite exhibits a larger surface area and superior adhesion capability onto demineralized enamel. Several studies have reported that nano-hydroxyapatite can increase enamel surface hardness, reduce mineral loss, and facilitate the deposition of new minerals on dental tissues (Wierichs, Wolf, Campus, & Carvalho, 2022; Amaechi, et al., 2022).

The characteristics of hydroxyapatite are heavily influenced by the synthesis method employed. Hydroxyapatite can be synthesized using either dry or wet methods. Dry methods, such as mechanochemical and solid-state synthesis, are relatively straightforward but face limitations in controlling particle size, homogeneity, and product purity. Conversely, wet methods, particularly the sol–gel method, enable precursor mixing at the molecular level, thereby yielding materials with smaller particle sizes, a more homogeneous particle distribution, and good crystallinity at relatively low synthesis temperatures (Xu, et al., 2022). These characteristics are crucial, as the particle size and crystallinity of hydroxyapatite directly influence its mineral deposition capability on demineralized enamel.

Research on nano-hydroxyapatite as an enamel remineralization agent has been widely reported. However, most studies still focus on evaluating remineralization effectiveness or material characterization in isolation. The correlation between the specific characteristics of sol-gel synthesized nano-hydroxyapatite, such as particle size and crystallinity, and its enamel remineralization effectiveness remains largely underreported. Furthermore, the development of sol-gel synthesized nano-hydroxyapatite into remineralization paste formulations is still relatively limited. Therefore, this study was conducted to synthesize nano-hydroxyapatite using the sol–gel method, characterize the resulting material, and evaluate its potential as an active ingredient in a remineralization paste for demineralized teeth. The novelty of this research lies in the development of a remineralization paste based on sol-gel synthesized nano-hydroxyapatite and the evaluation of its application on demineralized tooth enamel. This study is expected to contribute to the development of biocompatible and effective remineralization biomaterials for dental applications.

Methods

Materials

The materials used in this study included calcium hydroxide ($Ca(OH)_2$, 96% purity, Merck®), phosphoric acid (H_3PO_4, 85% concentration, Merck®), ammonium hydroxide (NH_4OH, 25% concentration, Merck®), and ethanol (96% concentration, Merck®). Milli-Q water was utilized throughout the hydroxyapatite synthesis process, while distilled water was used for the formulation of the paste. Additional ingredients for the paste formulation consisted of methylparaben (nipagin), sodium carboxymethyl cellulose (Na-CMC), glycerol, menthol, and citric acid 1 M. Human premolar teeth were obtained from the Pratama Al-Islam Clinic (Bandung, Indonesia).

Instrumentation

X-ray diffraction (XRD) PANalytical X'Pert PRO series PW3040/X0, X-ray fluoresence (XRF) ARL Quant'X EDXRF Analyzer – Thermo Scientific, Particle

Size Analyzer (PSA) Horiba Scientific type SZ-100, and Scanning Electron Microscope (SEM) Jeol type 6510.

Procedure

Hydroxyapatite Synthesis

Hydroxyapatite synthesis was performed according to the method reported by Türk et al. (Türk, et al., 2019). A calcium hydroxide solution was prepared by dissolving 1.85 g of $Ca(OH)_2$ powder in 25 mL of Milli-Q water, while a phosphoric acid solution was prepared by diluting 1 mL of 85% H_3PO_4 with 25 mL of Milli-Q water. The $Ca(OH)_2$ solution was then heated to 60 °C under continuous stirring because previous studies have shown that hydroxyapatite with a well-defined crystalline structure can be obtained within this temperature range during sol–gel synthesis. Subsequently, the H_3PO_4 solution was added dropwise into the $Ca(OH)_2$ solution, and stirring was continued for 30 minutes. Following this, 25% NH_4OH solution was added until the pH of the mixture reached 11. The resulting mixture was then aged at room temperature for 24 h until gel formation occurred. The formed gel was separated via filtration, washed with distilled water until a neutral pH was reached to promote hydroxyapatite formation and minimize the formation of secondary calcium phosphate phases. The washing step was performed to remove residual ions and unreacted precursors from the gel matrix. Drying at 105 °C for 6 hours was subsequently carried out to remove moisture prior to calcination, while calcination at 950 °C for 4 hours was intended to improve crystallinity and facilitate the formation of hydroxyapatite as the dominant phase.

Characterization of Hydroxyapatite

The synthesized hydroxyapatite was characterized using X-ray diffraction (XRD), X-ray fluorescence (XRF), and particle size analysis (PSA). XRD analysis was performed using a PANalytical X'Pert PRO PW3040/X0 diffractometer with Cu Kα radiation ($\lambda = 1.5406$ Å) to determine the crystalline phases and crystallinity of the synthesized hydroxyapatite. The degree of crystallinity was estimated from the ratio between the crystalline peak area and the total diffractogram area using Origin software. XRF measurements were carried out using an ARL Quant'X EDXRF Analyzer (Thermo Scientific) equipped with a Si(Li) detector to determine the elemental composition and Ca/P ratio. Particle size distribution was measured using a Horiba SZ-100 Particle Size Analyzer at a scattering angle of 90°. Hydroxyapatite powder was dispersed to a concentration of 0.01 wt% prior to measurement.

Based Hydroxyapatite Paste Synthesis

The hydroxyapatite paste was prepared following the procedure reported by Setyawati et al. (Setyawati & Silviana, 2019). The synthesized hydroxyapatite was weighed at 0.5 grams, then 1 gram of glycerol was added and stirred until uniformly dispersed. Subsequently, 0.25 grams of nipagin and 0.1 grams of NaCMC were dissolved in 1 mL hot distilled water. 0.05 grams of menthol was dissolved in a

small amount of ethanol and added to the mixture. All components were then thoroughly mixed until a homogeneous hydroxyapatite paste was obtained. NaCMC was used as a gelling agent, glycerol as a humectant, menthol as a flavoring agent, and methylparaben as a preservative to maintain formulation stability (Rowe, Sheskey, & Quinn, 2006).

Demineralization and Characterization

In this procedure, the premolar teeth were first prepared. The premolar teeth were obtained from the Pratama Al-Islam clinic (Bandung, Indonesia). The premolar teeth were cleaned and then sectioned with a carborundum disc, leaving only the crowns. The prepared premolar teeth were demineralized by soaking in a 1 M citric acid solution for one hour, then rinsed with distilled water. The demineralized teeth were then characterized using a scanning electron microscopy (SEM).

Remineralization and Characterization

The hydroxyapatite paste was applied to the demineralized premolars, left for one hour, and then washed with distilled water. The application procedure was repeated once daily for 14 consecutive days. Following the remineralization period, the specimens were characterized using a JEOL JSM-6510 SEM at a magnification of 2,000×.

Results and Discussion

Hydroxyapatite Synthesis

Hydroxyapatite was successfully synthesized via the sol–gel method using calcium hydroxide and phosphoric acid as precursors. During the synthesis process, the precursor mixture gradually transformed into a gel after 24 h of aging, indicating successful progression of the sol–gel reaction. Similar gel formation behavior has been reported during the sol–gel synthesis of hydroxyapatite (Türk, et al., 2019; Osuchukwu, Salihi,, Abdullahi, & Obada, 2022). The overall reaction can be represented as follows:

$$10Ca(OH)_2 + 6H_3PO_4 \rightarrow Ca_{10}(PO_4)_6(OH)_2 + 18H_2O \quad \text{..... (1)}$$

After filtration, washing, and drying, a white solid was obtained, suggesting the formation of a calcium phosphate-based material. Following calcination at 950 °C, the product appeared as a fine white powder. Similar observations have been reported for hydroxyapatite synthesized via the sol–gel method, where calcination contributes to phase stabilization and improved crystallinity (Türk, et al., 2019; Osuchukwu, Salihi,, Abdullahi, & Obada, 2022; Siswanto, Hikmawati, & Falentina, 2025). Although the visual appearance of the synthesized powder suggested successful hydroxyapatite formation, phase identification and purity could not be confirmed solely through visual observation. Therefore, further characterization using XRD, XRF, and PSA analyses was conducted to evaluate the structural, compositional, and particle-size properties of the synthesized material.

Characterization of Hydroxyapatite
X-Ray Diffraction (XRD)

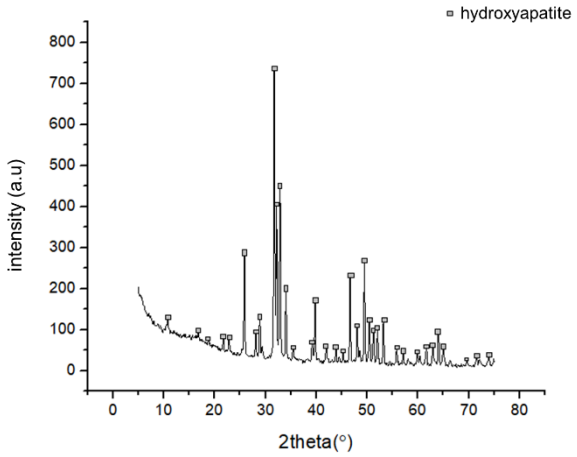


Figure 1. Diffractogram of XRD Analysis Results

Figure 1 presents the XRD diffractogram of the synthesized hydroxyapatite. Phase identification was performed by comparison with standard hydroxyapatite data from PDF/JCPDS No. 98-003-4457. The observed diffraction peaks showed good agreement with the characteristic peaks of hydroxyapatite, indicating successful formation of the target phase (Siswanto, Hikmawati, & Falentina, 2025; Türk, et al., 2019). A comparison of the major diffraction peaks of the synthesized hydroxyapatite with the reference pattern is presented in **Table 1**.

Table 1. Comparison of major diffraction peaks between synthesized hydroxyapatite and standard hydroxyapatite (PDF/JCPDS No. 98-003-4457)

2 theta Angle	
Standard	**Hydroxyapatite**
25.87°	25.85°
28.92°	28.85°
31.77°	31.71°
32.19°	32.17°
32.66°	32.87°
34.06°	34.04°
39.64°	39.77°
46.69°	46.68°
48.08°	48.04°

No additional crystalline impurity phases were detected within the detection limit of the XRD analysis. Furthermore, pattern matching using HighScore Plus software indicated that all major diffraction peaks corresponded to hydroxyapatite. Therefore, the synthesized material can be considered predominantly

hydroxyapatite without detectable crystalline secondary phases, although the presence of trace impurities or amorphous phases below the detection limit of XRD cannot be completely excluded (Cullity & Stock, 2014).

The lattice parameters obtained from XRD analysis were also comparable to those of standard hydroxyapatite (**Table 2**), suggesting that the synthesized material possessed a crystal structure consistent with hydroxyapatite. Minor differences between the synthesized and reference values may be attributed to synthesis conditions and instrumental factors.

Table 2. Comparison of lattice parameters between synthesized hydroxyapatite and standard hydroxyapatite (PDF/JCPDS No. 98-003-4457)

Lattice Parameter	Standard (Å)	Hydroxyapatite (Å)
a	9.4210	9.42300
b	6.8810	6.87550
c	18.8425	18.87200

Based on diffractogram processing using Origin software, the degree of crystallinity of the synthesized hydroxyapatite was approximately 36.5%. This result suggests that the synthesized material contains both crystalline and amorphous fractions. Since crystallinity is influenced by factors such as precursor composition, synthesis conditions, aging treatment, and calcination parameters, the obtained value should be regarded as an estimated rather than an absolute measurement (Trzaskowska, Vivcharenko, & Przekora, 2023; Siswanto, Hikmawati, & Falentina, 2025).

The average crystallite size calculated using the Debye–Scherrer equation was approximately 45.7 nm. Because this method is based on diffraction peak broadening, the calculated value represents an approximate crystallite size and may be affected by instrumental broadening and lattice strain (Monshi, Foroughi, & Monshi, 2012). Nevertheless, the obtained crystallite size falls within the nanometer range commonly reported for synthetic hydroxyapatite and is comparable to that of biological hydroxyapatite in human enamel (48–78 nm) (Islam, et al., 2025). The nanoscale crystallite size may facilitate interaction with demineralized enamel surfaces because of its relatively high surface area (Pepla, Besharat, Palaia, Tenore, & Migliau, 2014; Anil, Ibraheem, Meshni, Preethanath, & Anil, 2022).

X-Ray Fluorescence (XRF)

XRF analysis was performed to determine the elemental composition of the synthesized hydroxyapatite. The results showed that calcium (65.55%) and phosphorus (29.48%) were the predominant elements detected, accompanied by trace amounts of several other elements, including Al, Si, Te, Sb, Ge, and Br (**Table 3**). Based on the elemental composition data, the molar Ca/P ratio of the synthesized hydroxyapatite was calculated to be 1.72, which is slightly higher than the stoichiometric Ca/P ratio of pure hydroxyapatite (1.67). The stoichiometric ratio of

1.67 is widely recognized as the characteristic composition of hydroxyapatite and is commonly used as a reference in biomaterial applications (Anggresani, Perawat, Diana, & Sutrisno, 2020).

Table 3. Elemental composition of synthesized hydroxyapatite determined by XRF analysis

Element	Composition (%)
Ca	65.55
P	29.48
Al	0.49
Si	0.07
Te	0.0013
Sb	0.0011
Ge	0.0002
Br	0.0001

The slight increase in the Ca/P ratio suggests a minor deviation from the ideal stoichiometric composition. Such deviations may arise from variations in synthesis conditions, including precursor mixing efficiency, reaction kinetics, and ion loss during post-synthesis washing steps (Osuchukwu, Salihi,, Abdullahi, & Obada, 2022; Türk, et al., 2019). Nevertheless, the obtained Ca/P ratio remains close to the theoretical value and falls within the range commonly reported for synthetic hydroxyapatite (Rial, Gonzalez-Durruthy, Liu, & Ruso, 2021; Osuchukwu, Salihi,, Abdullahi, & Obada, 2022).

Furthermore, the XRD analysis confirmed hydroxyapatite as the dominant crystalline phase and did not reveal the presence of any crystalline secondary phases. Therefore, the observed deviation in the Ca/P ratio is unlikely to be associated with the formation of crystalline impurity compounds. Several trace elements, including Al, Si, Te, Sb, Ge, and Br, were detected at very low concentrations. However, their concentrations were negligible compared with those of calcium and phosphorus and are therefore unlikely to significantly affect the composition of the synthesized hydroxyapatite. Overall, the XRF results indicate that the synthesized material possesses an elemental composition that closely resembles that of stoichiometric hydroxyapatite.

Particle Size Analyzer (PSA)

PSA was performed to determine the particle size of the synthesized hydroxyapatite. The measurement results revealed that the hydroxyapatite had an average particle size of 344.2 nm. This size falls within the nanometer range (less than 1,000 nm) (Mohanraj & Chen, 2007; Rial, Gonzalez-Durruthy, Liu, & Ruso, 2021). Thus, the obtained material can be categorized as nano-hydroxyapatite particles.

The obtained particle size is larger than the crystallite size calculated from the XRD analysis, which was 45.7 nm. This discrepancy indicates that a single particle

measured by PSA is likely composed of multiple crystallites that have aggregated or agglomerated into larger particles. This phenomenon is commonly encountered in synthetic hydroxyapatite materials due to the high surface energy of nano-sized particles, which drives interparticle interactions (Rial, Gonzalez-Durruthy, Liu, & Ruso, 2021).

Nevertheless, the average particle size of 344.2 nm remains within the nanoscale range and may be favorable for enamel remineralization applications. Nano-sized hydroxyapatite particles generally exhibit a higher surface area than micrometer-sized particles, which can enhance their interaction with demineralized enamel surfaces and promote mineral deposition (Pepla, Besharat, Palaia, Tenore, & Migliau, 2014; Wierichs, Wolf, Campus, & Carvalho, 2022). Therefore, the PSA results indicate that the applied synthesis method successfully produced nano-hydroxyapatite particles with characteristics potentially suitable for remineralization-based biomaterial applications.

Hydroxyapatite Paste Synthesis

The synthesized hydroxyapatite was successfully formulated into a semi-solid paste intended for enamel remineralization. The resulting formulation exhibited a homogeneous appearance without visible phase separation, indicating adequate dispersion of hydroxyapatite particles within the paste matrix. The paste maintained a semi-solid consistency that allowed its application onto the enamel surface during the remineralization experiment. Similar hydroxyapatite-based paste formulations have been reported for enamel remineralization applications (Sari, Ramadhanti, Amalina, Ana, & Yusuf, 2022; Florea, et al., 2023).

Demineralization and Its Characteristics

Demineralization refers to the dissolution of mineral components of hydroxyapatite in hard dental tissues, including enamel, dentin, and cementum. This process is characterized by the loss of calcium and phosphate ions from the hydroxyapatite crystal lattice, leading to progressive weakening of the tooth structure (Enax, Fandrich, Schulze zur Wiesche, & Epple, 2024). In teeth, demineralization is primarily induced by acid exposure from dietary sources and bacterial metabolism in the oral environment (Abou Neel, et al., 2016; Xu, et al., 2022). The overall demineralization reaction of hydroxyapatite can be expressed as:

$$(Ca_{10}(PO_4)_6(OH)_2) + 8H^+ \rightarrow 10Ca^{2+} + 6(HPO_4^{2-}) + 2H_2O.. (2)$$

In this study, demineralization of premolar teeth was induced by immersion in 1 M citric acid solution (pH 3.57) for 1 hour. This acidic condition is below the critical pH of hydroxyapatite (≈5.5), allowing enamel mineral dissolution through acid-induced hydroxyapatite degradation (Abou Neel, et al., 2016; O'Hagan-Wong, Enax, Meyer, & Ganss, 2022). SEM analysis (**Figure 2a**) revealed marked morphological alterations after acid treatment, characterized by a rough, irregular,

and porous enamel surface. Compared with intact enamel, the increased porosity and surface defects indicate substantial mineral loss resulting from hydroxyapatite dissolution. Similar morphological features have been reported for demineralized enamel in previous studies (Xu, et al., 2022; Abou Neel, et al., 2016). The observed surface characteristics confirm that the demineralization procedure successfully generated an enamel lesion model suitable for subsequent remineralization evaluation.

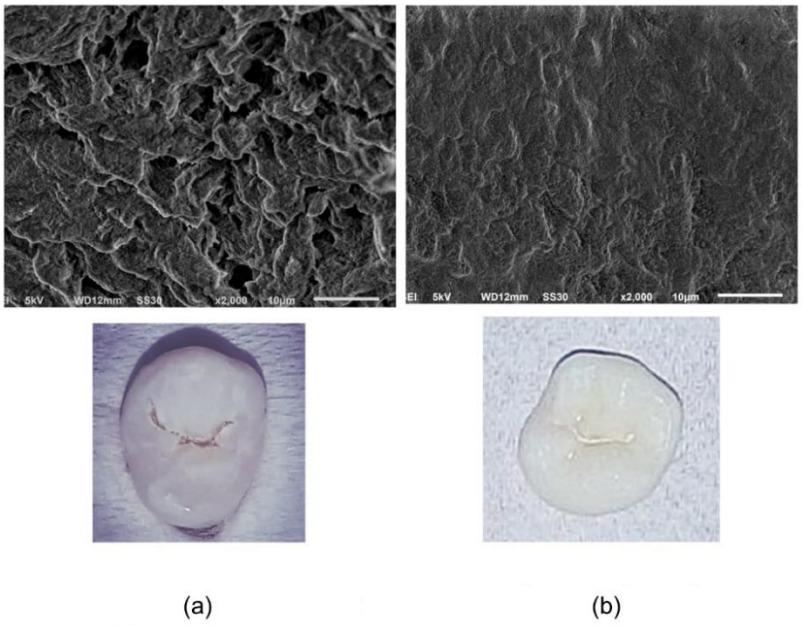


Figure 2. SEM Analysis Results of (a) Demineralized Teeth and (b) Remineralized Teeth

Remineralization and Its Characteristics

Remineralization was evaluated after 14 consecutive days of hydroxyapatite paste application. Following treatment, the enamel surface exhibited a more uniform appearance with reduced porosity compared to the demineralized condition. Similar morphological recovery following hydroxyapatite application has been widely reported in recent studies on enamel biomimetic remineralization (Anil, Ibraheem, Meshni, Preethanath, & Anil, 2022; Florea, et al., 2023).

SEM analysis (**Figure 2b**) revealed a reduction in microcavities and surface irregularities compared with the demineralized enamel, indicating partial occlusion of enamel defects. The enamel surface also appeared more uniform and less porous after 14 days of hydroxyapatite paste application. These observations suggest that hydroxyapatite deposition occurred on the demineralized enamel surface and contributed to partial surface restoration. Similar morphological improvements have been reported following the application of nano-hydroxyapatite to demineralized enamel (Anil, Ibraheem, Meshni, Preethanath, & Anil, 2022; Florea, et al., 2023). The observed changes are similar to those reported for previously proposed remineralization mechanisms involving calcium-phosphate mineral

deposition and biomimetic interaction between hydroxyapatite particles and enamel (Wierichs, Wolf, Campus, & Carvalho, 2022; O'Hagan-Wong, Enax, Meyer, & Ganss, 2022). In addition, the treated enamel appeared visually brighter than the demineralized sample. However, this observation was qualitative and may have been influenced by surface morphology and light scattering effects. Therefore, the primary evidence of remineralization in this study is based on the SEM-observed reduction in porosity and microcavity formation, indicating partial recovery of the enamel surface after hydroxyapatite paste application.

Conclusion

Hydroxyapatite was successfully synthesized via the sol–gel method and formulated into a hydroxyapatite-based paste for enamel remineralization applications. The synthesized material exhibited a hydroxyapatite crystalline phase with a near-stoichiometric Ca/P ratio of 1.72 and a nanoscale particle size of 344.2 nm, indicating its suitability for biomimetic dental applications. Application of the hydroxyapatite paste on demineralized enamel resulted in noticeable morphological improvements, including reduced surface porosity and increased surface uniformity as observed by SEM analysis. These changes suggest partial remineralization of the enamel surface, although the evaluation was limited to morphological assessment. Overall, the study demonstrates the potential of sol–gel-derived nano-hydroxyapatite as a biomaterial for enamel surface repair. The findings highlight its capability to interact with demineralized enamel and support early-stage remineralization processes. Further quantitative and long-term studies are required to fully validate its clinical effectiveness and durability.

Acknowledgements

The authors would like to acknowledge Pratama Al-Islam Clinic for providing the premolar teeth utilized in this research.

References

Abou Neel, E. A., Aljabo, A., Strange, A., Ibrahim, S., Coathup, M., Young, A. M., . . . Mudera, V. (2016). Demineralization–remineralization dynamics in teeth and bone. *International journal of nanomedicine*, 4743-4763. doi:https://doi.org/10.2147/IJN.S107624

Amaechi, B. T., Farah, R., Liu, J. A., Phillips, T. S., Perozo, B. I., Kataoka, Y., . . . Enax, J. (2022). Remineralization of molar incisor hypomineralization (MIH) with a hydroxyapatite toothpaste: an in-situ study. *BDJ open*, *8*(1), 33.

Anggresani, L., Perawat, S., Diana, F., & Sutrisno, D. (2020). Pengaruh variasi perbandingan mol Ca/P dalam pembuatan hidroksiapatit dari tulang ikan tenggiri (*Scomberomorus guttatus*). *Jurnal Farmasi Higea, 12*(1), 55-64. doi:http://dx.doi.org/10.52689/higea.v12i1.264

Anil, A., Ibraheem, W. I., Meshni, A. A., Preethanath, R. S., & Anil, S. (2022). Nano-hydroxyapatite (nHAp) in the remineralization of early dental caries: a scoping review. *International journal of environmental research and public health, 19*(9), 5629.

Cullity, B. D., & Stock, S. R. (2014). *Elements of X-ray Diffraction.* Upper Saddle River: Pearson.

Enax, J., Fandrich, P., Schulze zur Wiesche, E., & Epple, M. (2024). The remineralization of enamel from saliva: A chemical perspective. *Dentistry Journal, 12*(11), 339.

Florea, A. D., Pop, L. C., Benea, H. R., Tomoaia, G., Racz, C. P., Mocanu, A., . . . Tomoaia-Cotisel, M. (2023). Remineralization Induced by Biomimetic Hydroxyapatite Toothpastes on Human Enamel. *Biomimetics, 8*(6), 450.

Guntermann, L., Rohrbach, A., Schäfer, E., & Dammaschke, T. (2022). Remineralization and protection from demineralization: effects of a hydroxyapatite-containing, a fluoride-containing and a fluoride- and hydroxyapatite-free toothpaste on human enamel in vitro. *Head & face medicine, 18*(1), 26. doi:https://doi.org/10.1186/s13005-022-00330-5

Islam, M. A., Hossain, N., Hossain, S., Khan, F., Hossain, S., Arup, M. M., . . . Rahmad, M. M. (2025). Advances of hydroxyapatite nanoparticles in dental implant applications. *International Dental Journal, 75*(3), 2272-2313. doi:https://doi.org/10.1016/j.identj.2024.11.020

Mohanraj, V. J., & Chen, Y. (2007). Nanoparticles - A review. *Tropical Journal of Pharmaceutical Research, 5*(1), 561–573. doi:https://doi.org/10.4314/tjpr.v5i1.14634

Monshi, A., Foroughi, M. R., & Monshi, M. R. (2012). Modified Scherrer equation to estimate more accurately nano-crystallite size using XRD. *World Journal of Nano Science and Engineering, 2*(3), 154-160. doi:http://dx.doi.org/10.4236/wjnse.2012.23020

O'Hagan-Wong, K., Enax, J., Meyer, F., & Ganss, B. (2022). The use of hydroxyapatite toothpaste to prevent dental caries. *Odontology, 110*(2), 223-230.

Osuchukwu, O. A., S. A., Abdullahi, I., & Obada, D. O. (2022). Synthesis and characterization of sol–gel derived hydroxyapatite from a novel mix of two natural biowastes and their potentials for biomedical applications. *Materials Today: Proceedings, 62*, 4182-4187. doi:https://doi.org/10.1016/j.matpr.2022.04.696

Pepla, E., Besharat, L. K., Palaia, G., Tenore, G., & Migliau, G. (2014). Nano-hydroxyapatite and its applications in preventive, restorative and regenerative dentistry: a review of literature. *Annali di stomatologia, 5*(3), 108.

Rial, R., Gonzalez-Durruthy, M., Liu, Z., & Ruso, J. M. (2021). Advanced materials based on nanosized hydroxyapatite. *Molecules, 26*(11), 3190. doi:https://doi.org/10.3390/molecules26113190

Rowe, R. C., Sheskey, P. J., & Quinn, M. E. (2006). *Handbook of pharmaceutical excipients.* London: Pharmaceutical press.

Sari, M., Ramadhanti, D. M., Amalina, R., Ana, I. D., & Yusuf, Y. (2022). Development of a hydroxyapatite nanoparticle-based gel for enamel remineralization—A physicochemical properties and cell viability assay analysis. *Dental Materials Journal, 41*(1), 68-77.

Setyawati, A., & Silviana, F. (2019). Pengaruh pasta cangkang telur ayam negeri terhadap email gigi. *Denta Jurnal Kedokteran Gigi, 13*(2).

Siswanto, Hikmawati, D., & Falentina, W. D. (2025). The Role of Calcination Temperature Variation in The Sol–Gel Synthesis of Hydroxyapatite. *Indonesian Applied Physics Letters, 6*(1), 8-13. doi:https://doi.org/10.20473/iapl.v6i1.84056

Trzaskowska, M., Vivcharenko, V., & Przekora, A. (2023). The impact of hydroxyapatite sintering temperature on its microstructural, mechanical, and biological properties. *International journal of molecular sciences, 24*(6), 5083. doi:https://doi.org/10.3390/ijms24065083

Türk, S., Altınsoy, İ., Çelebi Efe, G., Ipek, M., Özacar, M., & Bindal, C. (2019). Effect of solution and calcination time on sol-gel synthesis of hydroxyapatite. *Journal of Bionic Engineering, 16*(2), 311-318. doi:https://doi.org/10.1007/s42235-019-0026-3

Wierichs, R. J., Wolf, T. G., Campus, G., & Carvalho, T. S. (2022). Efficacy of nano-hydroxyapatite on caries prevention—a systematic review and meta-analysis. *Clinical oral investigations, 26*(4), 3373-3381. doi:https://doi.org/10.1007/s00784-022-04390-4

Xu, J., Shi, H., Luo, J., Yao, H., Wang, P., Li, Z., & Wei, J. (2022). Advanced materials for enamel remineralization. *Frontiers in bioengineering and biotechnology, 10*, 985881. doi:10.3389/fbioe.2022.985881